Hu, Fang; Hu, Huiping; Yang, Jinpeng; Luo, Yuqing; Lundstrom, Mari; Ji, Guangfu; Hu, Jiugang

Preferential extraction of Ni(II) over Co(II) by arylsulphonic acid in the presence of pyridinecarboxylate ester

Published in:
Journal of Molecular Liquids

DOI:
10.1016/j.molliq.2019.111253

Published: 01/10/2019

Document Version
Peer-reviewed accepted author manuscript, also known as Final accepted manuscript or Post-print

Preferential extraction of Ni(II) over Co(II) by arylsulphonic acid in the presence of pyridinecarboxylate ester: Experimental and DFT calculations

Fang Hu[1,2,3], Huiping Hu[1,2,*], Jinpeng Yang[1,2], Yuqing Luo[1,2], Mari Lundstrom[3], Guangfu Ji[4], Jiugang Hu[1,2,*]

[1] College of Chemistry and Chemical Engineering, Central South University, Changsha 410083, Hunan, China.

[2] Hunan Provincial Key Laboratory of Efficient and Clean Utilization of Manganese Resources, Central South University, Changsha 410083, Hunan, China.

[3] Hydrometallurgy and Corrosion, Department of Chemical and Metallurgical Engineering (CMET), School of Chemical Engineering, Aalto University, P.O. Box 16200, FI-00076 AALTO, Finland.

[4] Institute of Fluid Physics, Chinese Academy of Engineering Physics, Mianyang 62900, Sichuan, China.

Corresponding Authors

E-mail: hujiugang@csu.edu.cn; phuhuiping@126.com; Tel/Fax: +86 7361 88879616

ABSTRACT:

Selective extraction of Ni(II) from base metals is a critical step in the direct nickel synergistic extraction process. Significant synergistic effect and preferential extraction of Ni(II) over Co(II) were observed by using the synergistic extractant containing dinonylnaphthalene sulfonic acid (HDNNS) and 2-ethylhexyl 4-pyridinecarboxylate ester (ligand L) in Escaid 110. The selectivity sequence followed the order: Ni(II)>Co(II)>Al(III)>Mg(II)>Fe(III). In order to elucidate the separation difference between Ni(II) and Co(II) which had similar chemical properties, statistical thermodynamics analysis and relativistic density functional theory (DFT) calculations were applied to provide the selective mechanism from both macroscopic and microscopic perspectives. The synergistic extraction diagrams showed that the optimum molar ratio of HDNNS and the ligand L was at 1:2 for Ni(II) and Co(II) extraction, and statistical thermodynamics analysis indicated that the overall extraction process was endothermic. According to DFT calculation results, the optimized geometries of the Ni(II) and Co(II) complexes were in accordance with the crystallographical data. The thermodynamical examination for the Ni and Co extraction was further conducted using a thermodynamical cycle. The difference in the change of Gibbs free energies for the formation of the Ni(II) complex was more negative than that of the Co(II) complex, which was in agreement with the experimental data. It could be concluded that the synergistic extractant had a higher affinity for Ni(II) than Co(II), which might account for the preferential extraction of Ni(II) over Co(II). The results established a computational model capable of predicting the selectivity order of metal ions, which would provide new insights into the separation mechanism of Ni(II) and Co(II) with synergistic extractants.

Keywords: Separation mechanism; Synergistic extractant; DFT calculation; Thermodynamical cycle; Nickel

1. Introduction

As energy demand continues to grow, nickel and cobalt are amongst the most important non-ferrous metals. The separation of Ni(II) and Co(II) has aroused commonly concern since Ni(II) and Co(II) showed close chemical properties, such as similar oxidation state, ionic radii, and coordination numbers. The extraction and the separation of Ni(II) and Co(II) have been extensively studied using diverse extractants and some industrial processes have been in operation. The general route was to selectively extract Co(II) against Ni(II) by organophosphorus extractants. In recent years, lateritic nickel ores with low grade represent an alternative source because the traditional sulfide ores are fast exhausted. However, specific selective extractant for Ni(II) from laterite leachates remained scarce so that the separation and the concentration of Ni(II) and Co(II) present technical challenges.

In the industrial practice of hydrometallurgical treatment, synergistic solvent extraction (SSX) was favored for the recovery of nickel from laterite leachates. Cheng et al have systematically reviewed the synergistic systems for direct and selective extraction of Ni(II) from acidic polymetallic media [1-3]. Generally, the direct Ni(II) SSX systems could be classified according to O-donor acidic ligands, mainly including organophosphorus acids [4, 5], carboxylic acids [2, 6], or aryl sulfonates [7, 8] in combination with N-donor basic ligands such as Lix®63 (the active extractant is 5,8-diethyl-7-hydroxy-6-dodecanone oxime) or pyridine- carboxylate ester. In terms of pH_{50}, the synergistic extractant systems containing aryl sulfonates and pyridine-based ligands were found to selectively extract Cu(II), Ni(II) and Co(II) over

Fe(III), Mn(II), Ca(II), Mg(II) and Al(III) from highly acidic polymetallic medium at pH lower to 0.5, which made the direct separation of Ni(II) and Co(II) from acidic solutions possible without the prior removal of impurities, such as Fe(III) and Al(III), by intermediate neutralization or precipitation steps [9, 10]. Interestingly, Ni(II) seemed preferable to be extracted by the synergistic extractants containing aryl sulfonates and pyridine-based ligands mentioned above than that of Co(II) under the same extraction conditions, which indicated totally different separation performance from that of organophosphorus extractants. Hence, it is desirable to investigate the separation mechanism of Ni(II) towards Co(II) with the synergistic extractant systems.

Some authors have tried to elucidate the synergistic mechanism for Ni(II)/Co(II) separation with the extractants containing aryl sulfonates and pyridine-based ligands [11-15]. Based on the macroscopic slope analysis, stoichiometry of Ni(II) and Co(II) complexes with synergistic extractants containing HDNNS and BNPP (2,6-bis-[5-n-nonylpyrazol-3-yl] pyridine) was determined, where the formation of Ni(II) or Co(II) complex occurred with a metal: BNPP:HDNNS stoichiometric ratio of 1:2:1 [12]. Okewole et al. explored a synergistic extractant containing HDNNS and bidentate aromatic nitrogen donor ligand 1-octyl-2-(2′-pyridyl) imidazole (OPIM) which resulted with a chelating character for selective Ni(II) extraction, and the authors attributed the driving factor for the extraction priority of Ni(II) to the kinetics of the complexation based on spectrophotometric titrations [13]. Recently, our research group has illustrated the geometries of metal complexes with aryl sulfonates

and monodentate aromatic nitrogen donor ligand 2-ethylhexyl 4-pyridinecarboxylate ester (the ligand L) from combined single crystal X-ray diffraction of model complexes and spectra studies [14-17], and it was found that both of Ni(II) and Co(II) were coordinated by four oxygen atoms from water molecules and two nitrogen atoms from the ligand L while hydrogen-bonded interactions existed between the coordinated water molecules and sulfonic oxygen atoms from deprotonated HDNNS. The same coordination chemistry of Ni(II) and Co(II) complexes was, however, not sufficient to explain the extraction preference. Thus, the extraction preference for Ni(II) towards Co(II) with the synergistic extractant remained as an open question.

Theoretically, the equilibrium constant is related to the free energy difference between the reactants and the products of the reaction, ΔG_{ext}. It has been broadly studied about the effect of different thermodynamical stabilities of extractable complexes (of the same composition and structure) of two metal ions on the selectivity of their separation ($\ln SF = -\frac{\Delta\Delta G_{ext}}{RT}$). Theoretical approach such as density functional theory (DFT) calculation has already enabled to provide a fine description of the chemical stability and estimate the atomic-level structure and energy of metal ion complexes [18]. Similar procedures were employed to examine the selective extraction of Am(III)/Cm(III) from Eu(III) by dithiophosphinic acids [19, 20]. DFT calculation on Am(III)/Ln(III) and Am(III)/Eu(III) separation indicated that the stabilization of metal ions by the complexation in aqueous solutions was required to reproduce the experimental separation behaviors [21, 22]. However, theoretical investigations on Ni(II)/Co(II) liquid-liquid extraction using a synergistic extraction

system with two or more ligands are rare. Herein, we devoted to the validation of the coordination structure of metal complexes, showing that the preferential extraction of Ni(II) over Co(II) directly from the difference in the energies between the synergistic extractants and metal ions.

In this work, a comprehensive study of the separation behavior and mechanism for Ni(II) and Co(II) with synergistic extractant containing HDNNS and the ligand L was presented. The pH isotherm of Ni(II) and Co(II) against impurity metal cations was obtained, and the extraction behaviors of Ni(II) and Co(II) under different extractant concentrations and temperature were compared. Along with experimental studies, the effects were also being put forward for the understanding of the structure, bonding and thermodynamics of Ni(II) and Co(II) with the synergistic extractants using quantum chemical calculations. The correlation between microscopic properties and the extractability of Ni(II) and Co(II) with the synergistic extractant was discussed after validating the reproducibility of the experimental selectivity for Ni(II)/Co(II) ions. This study may provide some useful information for understanding the complexation and separation mechanism of Ni(II) and Co(II) with the synergistic extractants, which helps us to promote the design and modification of novel synergistic extraction system with high selectivity based on related ligands.

2. Experiments

2.1 Materials and chemicals

HDNNS, which was supplied by Shanghai JiaChen Chemical Co., Ltd, was

130 further purified according to our previous study. $NiSO_4$, $CoSO_4$, $MgSO_4$, $Al_2(SO_4)_3$
131 and $Fe_2(SO_4)_3$ were obtained from Sinopharm Chemical Reagent Co., Ltd.
132 2-Ethylhexyl 4-pyridinecarboxylate ester (ligand L), was synthesized following the
133 procedure described elsewhere [23]. Escaid 110 (200-248 ºC fraction hydrocarbon
134 fluid with 99.5% aliphatic content) was purchased from ExxonMobil Chemical and
135 used as diluents without further purification. Other chemicals were of analytical grade.
136 The structure of the ligand L and HDNNS is shown in Figs. 1a and 1b, respectively.
137 For avoiding the time-intensive quantum chemical calculations, a methyl group is
138 used to replace the long alkyl chain for both ligand L and HDNNS, as shown in Figs.
139 1c and 1d, respectively.

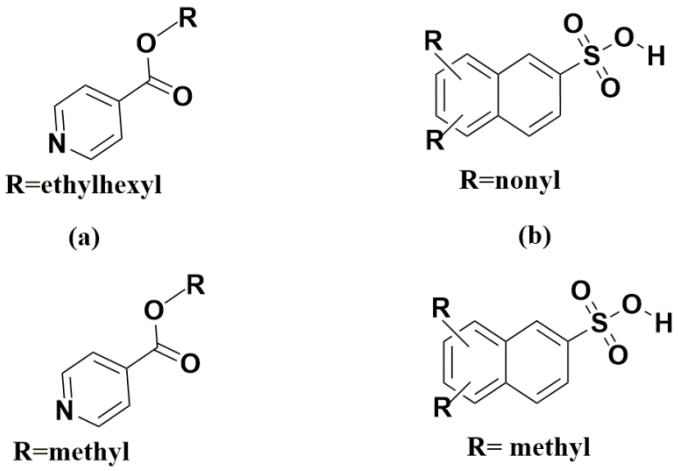

140

141 Fig. 1 The structures of 4-pyridinecarboxylate esters (a and c) and naphthalene
142 sulfonic acids (b and d).

143

144 **2.2 Solvent extraction procedure**

145 The initial aqueous phases containing 0.02 $mol \cdot L^{-1}$ metal ions (separately) in 0.5
146 $mol \cdot L^{-1}$ Na_2SO_4 supporting electrolyte (to provide a relatively constant ionic strength)

were prepared for pH distribution isotherm. Besides, the acidic solution containing 0.09 mol·L^{-1} Ni(II) or 0.09 mol·L^{-1} Co(II) in 0.5 mol·L^{-1} Na_2SO_4 supporting electrolyte was prepared for solvent extraction condition experiments, respectively. The initial pH of stored Ni(II) and Co(II) solutions was adjusted to 1.95 by concentrated H_2SO_4 or NaOH solution. Fresh organic phase was prepared by dissolving weighed quantities of HDNNS and the ligand L in Escaid 110 at a constant molar ratio of 1:2 (HDNNS/ligand L). The lean organic phase was pre-equilibrated with NaOH solution for 15min. Extraction measurements were performed in thermostat vessels at an A/O ratio of 1:1 and 25.0±0.1 °C. After equilibrated enough, the mixture was taken out and separated by centrifugation as soon as possible. The metal concentration in the aqueous phase was determined by inductively coupled plasma-atomic emission spectrometry (ICP-AES, Perkin Elmer 5300DV America). The metal concentration in the loaded organic phase was calculated by mass balance.

The extraction efficiency, E, was defined as,

$$E = \frac{[M]_o V_o}{[M]_o V_o + [M]V} \times 100\% \quad (1)$$

The distribution coefficient of Ni(II) or Co(II), D_{Me}, was defined as,

$$\mathrm{D_{Me}} = \frac{[M]_o}{[M]} \quad (2)$$

While $[M]_o$ and $[M]$(mol·L^{-1}) were the Ni(II) or Co(II) concentration in the loaded organic phase and the aqueous phase after equilibrium, respectively. V_o and V (L) were the respective volumes of the loaded organic phase and the aqueous phase.

2.3 DFT calculation details

All the calculations were performed by using unrestricted density functional theory (DFT) method with the hybrid functional B3LYP [24, 25], as implemented in Gaussian 03 software package [26]. The 6-311G(d) basis set was adopted for light atoms including H, C, N, O and S atoms. Ni(II) and Co(II) were modeled with the small core Stuttgart relativistic effective core potential with its associated basis set. The geometric configurations of Ni(II) and Co(II) complexes were optimized in the gas phase without symmetry constraints. The stationary points on the potential energy surfaces were validated as energy minima rather than saddle points using analytical frequency analysis at the same level of theory. Based on the optimized structure in the gas phase, the single point energy (E), enthalpy (H), entropy(S) , and Gibbs free energy (G) were calculated at the same level of theory.

The solvation energy is considered as the change in Gibbs free energy when an ion or molecule is transferred from the gas phase into a solution [27]. The development of dielectric continuum solvent models has facilitated to deliver accurate change values of the Gibbs free energies for chemical reactions in the condensed phase in a computationally efficient manner [28]. Estimates of the solvation effects were computed using the SMD continuum solvation model implemented in Gaussian 03 with radii and nonelectrostatic terms from A.V. Marenich and co-workers' SMD model [29]. The solute was immersed in a shape adapted isotropic polarizable continuum, parametrized with the value of solvent dielectric constants (ε) 78.3553 and 4.7113 for simulation of water (H_2O) and the solvent $CHCl_3$, respectively. The

191 solvation effects were calculated with geometries re-optimized in aqueous solution,
192 resulting in solvation energy.
193
194 **3. Results and discussion**
195 **3.1 Extraction selectivity of metal ions**
196 The pH isotherms for the extraction of Ni(II), Co(II) and some relevant base
197 metal cations (0.02 mol·L^{-1} each, separately) were conducted by using the synergistic
198 extractant containing 0.25 mol·L^{-1} HDNNS and 0.5 mol·L^{-1} ligand L in Escaid 110 at
199 an O/A ratio of 1:1 and 25 °C. For the present solvent extraction system, the Ni(II)
200 and Co(II) extractions can generally be written as:
201 $$M_{(aq)} + aL_{(org)} + bHN_{(org)} = [M \cdot L_a \cdot N_b]_{(org)} + bH^+_{(aq)} \quad (3)$$
202 Where M=Ni(II) or Co(II), HN=HDNNS, and N=deprotonated HDNNS.
203 $$K_{ex1} = \frac{[M \cdot L_a \cdot N_b]_{(org)}[H^+_{(aq)}]^b}{[M_{(aq)}][L_{(org)}]^a[HN_{(org)}]^b} \quad (4)$$
204 Then, $$\log D = \log K_{ex1} + b\,pH_e + a\log[L_{(org)}] + b\log[HN_{(org)}] \quad (5)$$
205 Where K_{ex1} is the equilibrium coefficient of Eq.3 and is a constant at a given
206 temperature. The mathematical relationship between the distribution coefficient
207 values and pH_e, the plots of log$D$ vs. pH_e for related metal cations were obtained
208 correspondingly. It can be seen from Fig. 2 that with the increase of equilibrium pH,
209 the extraction efficiencies of Ni(II) and Co(II) increase rapidly, while the extraction of
210 other base metal cations appears rather slow increase trends, especially Fe(III) and
211 Mg(II) at low pH value. The selectivity sequence at pH lower than 2.0 follows the
212 order (pH_{50} values in parentheses): Ni (1.34)>Co (2.12)>Al (3.47)>Mg (4.80). With

constant concentration of HDNNS and the ligand L at given temperature, values '*b*' in Eq.5 can be obtained as around 1 for Ni(II) and Co(II) as the slope of a plot of log*D* vs. pH_e, indicating that cation exchange reaction occurs during the extraction process. The selective behavior of Ni(II) over other base metal ions parallels the situation reported previously for Ni(II) extraction with synergistic extractants of sulphonic acids and pyridine-based ligands [8]. The enhancements of Ni(II) and Co(II) extraction are presumed to be correlated with the interaction between metal ions and the synergistic extractant containing HDNNS and the ligand L, compared with the extraction of Mg(II), Fe(III) and Al(III).

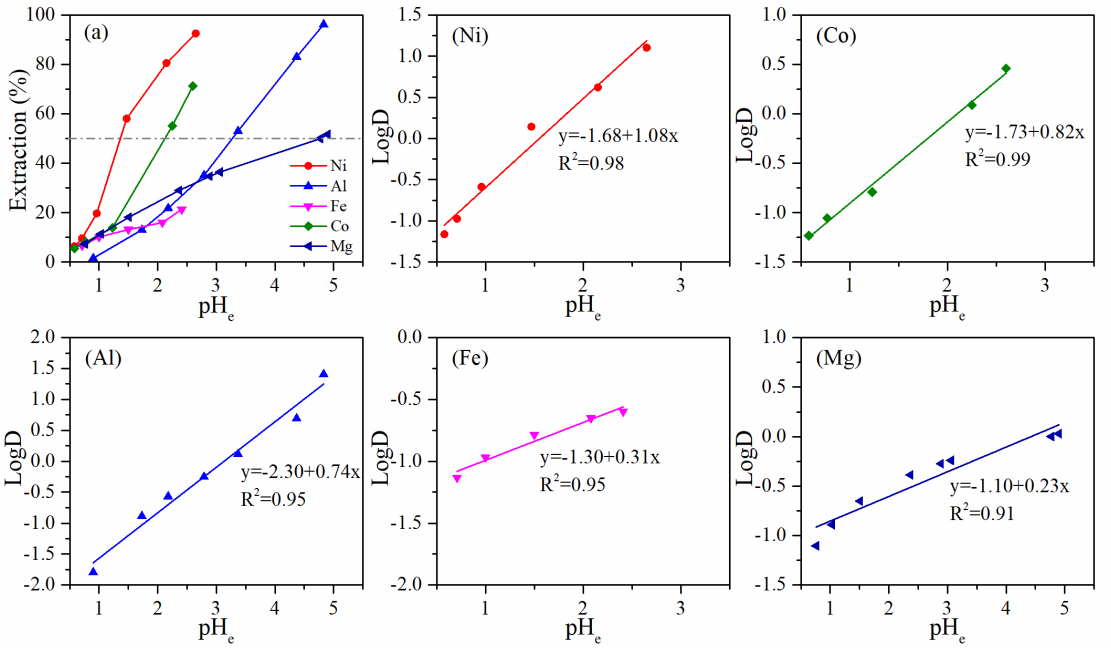

Fig. 2 pH isotherms and Log*D* vs. pH_e for metal cations (0.02 mol·L^{-1} each, separately) from 0.25 mol·L^{-1} sodium sulphate media with the synergistic extractant containing 0.25 mol·L^{-1} HDNNS and 0.5 mol·L^{-1} ligand L at an O/A ratio of 1:1 and 25 °C.

3.2 Extraction stoichiometry

The stoichiometry of the Ni(II) and Co(II) extraction was conducted by the synergistic extraction diagrams under requisite molar fraction of the ligand L (X_L, calculated as $[L_{(org)}]/([L_{(org)}]+[HN_{(org)}])\times100\%$) in the synergistic extractant while the total molar concentration of HDNNS and ligand L were kept at 0.75 mol·L^{-1}. The plots of log*D* versus the molar fraction of the ligand L, X_L, were presented in Fig. 3a. It can be seen that the maximum extractions for Ni(II) and Co(II) occur at X_L =66.7%, indicating that the optimum molar ratio of HDNNS and the ligand L is at 1:2. In addition, the possible stoichiometric ratio for the extracted Ni(II) or Co(II) complex in the organic phase was deduced as metal: HDNNS: L of 1:1:2 from combined crystal X-ray data of model complexes and spectra studies reported previously [14, 16], indicating that one HDNNS molecule and two ligand L are involved in the extraction of Ni(II) or Co(II) complex. Therefore, the relation of the 'a' and 'b' in Eq.5 is approximated as 'a=2b'. Then the effects of the total concentration of the synergistic extractant (with the optimum molar ratio of HDNNS and the ligand L at 1:2) on the Ni(II) and Co(II) extraction were investigated, which is presented in Fig. 3b. It is found that when the concentration of HDNNS ranges from 0.1 mol·L^{-1} to 0.4 mol·L^{-1}, the extraction efficiency of Ni(II) increases from 21.3% to 80.8%, and the extraction efficiency of Co(II) increases from 9.3% to 40.8%. The calculated distribution coefficients of Ni(II) and Co(II) ranges from -0.57 to 0.62 and from -0.98 to -0.16, respectively. According to Eq.5, with fixed molar ratio of HDNNS and the ligand L at 298 K and pH_e=1.95, values 'K_{ex1}' can be obtained as the intercepts of plots of log*D* vs. log $[HN_{(org)}]$. The corresponding changes of the Gibbs free energies for the Ni(II)

and Co(II) extractions can be calculated as -31.11 and -16.33 kJ·mol^{-1}, where the difference value in the Gibbs free energy change between the Ni(II) and Co(II) extractions is -14.78 kJ·mol^{-1}.

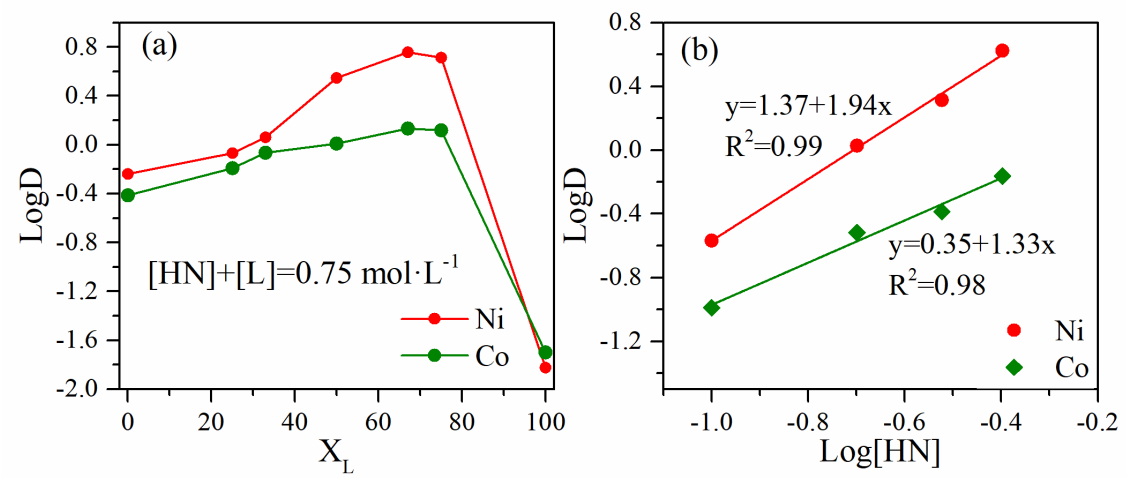

Fig. 3 Distribution coefficient for Ni(II) and Co(II) from 0.5 mol·L^{-1} Na_2SO_4 supporting electrolyte with synergistic extractant with fixed total molar concentration (a) and fixed molar ratio of HDNNS/ligand L at 1:2 (b) in Escaid 110 at an O/A ratio of 1:1 and 25 °C.

3.3 Effect of temperature

The extraction behaviors of Ni(II) and Co(II) were carried out at the temperature ranged from 298 K to 318 K, respectively. Generally, the extraction efficiencies of Ni(II) and Co(II) increase with the rise of temperature, indicating that increasing temperature is beneficial for the extraction of Ni(II) and Co(II) from aqueous solutions with the synergistic extractant containing HDNNS and the ligand L. In order to calculate the extraction thermodynamics parameters, the fitting straight lines were also presented in Fig.4. As shown in Fig. 4, increasing temperature causes a decrease in the distribution coefficients of Ni(II) and Co(II). The slopes of the fitting straight

lines are -0.865 and -0.972 for the Ni(II) and Co(II) extractions, respectively. The enthalpy change (ΔH) of the extraction reaction can be calculated by the Van't Hoff equation as follows,

$$\frac{\partial \log D}{\partial(^1/_T)} = -\frac{\Delta H}{2.303RT} \quad (6)$$

The enthalpy change values for the Ni(II) and Co(II) extraction reactions (correspondingly abbreviated as ΔH_{Ni} and ΔH_{Co}) were found to be 16.58 and 18.61 kJ·mol^{-1}, respectively. Accordingly, the enthalpy change value of the Ni(II) extraction is 2.03 kJ·mol^{-1} lower than that of the Co(II) extraction. The comparison of the enthalpy change values for the Ni(II) and Co(II) extraction reactions would reflect the influence of temperature on extraction reactions and discover the difference between the Ni(II) and Co(II) extractions from statistical thermodynamics aspects. To assess the randomness during the extraction process, the entropy changes can be calculated based on the obtained changes of Gibbs free energy and the enthalpy at given temperatures. The entropy changes for the Ni(II) and Co(II) extraction reactions at 298 K are obtained as -159.96 and -117.20 J·K^{-1}, respectively.

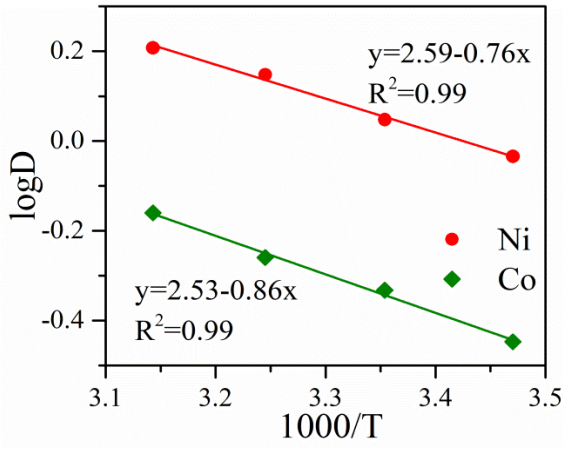

Fig. 4 Distribution coefficients for Ni(II) and Co(II) from 0.5 mol·L^{-1} Na_2SO_4

284 supporting electrolyte with the synergistic extractant containing 0.25 mol·L^{-1} HDNNS
285 and 0.5 mol·L^{-1} the ligand L in Escaid 110 at an O/A ratio of 1:1 and 25 °C.

286 The calculated difference in Gibbs free energy changes between the Ni(II) and
287 Co(II) extraction reactions (-14.78 kJ·mol^{-1}), indicates greater thermodynamic
288 stability for the Ni(II) extraction than that for the Co(II) extraction. However, the
289 bonding information from the predominating metal complexes still remains unknown.
290 Detailed microscopic structural analysis could further afford atomic-level insights on
291 the metal-ligand bonding as the origin of the preferential extraction of Ni(II) to Co(II).

292

293 **3 .4 Optimized geometries for Ni(II) and Co(II) complexes**

294 In our previous work, by single crystal structure studies of model complexes, the
295 coordination chemistry of Ni(II) and Co(II) extraction has been illustrated and found
296 that metal complexes with similar coordination configuration could be formed for
297 both Ni(II) and Co(II) in the organic phase [14, 16]. Herein, quantum chemical
298 calculations were used for better understanding the extractability of Ni(II) and Co(II).
299 The input geometry of the metal complexes for the DFT calculations was generated
300 from the single crystal X-ray data obtained with short chain analogs of the synergistic
301 extractant. Besides, the methyl group was used to replace alkyl carbon chains in
302 HDNNS and the ligand L, respectively. The geometries of the metal complexes
303 $Ni[L_2(H_2O)_4](DNNS)_2$ and $Co[L_2(H_2O)_4](DNNS)_2$ were optimized in the gas phase
304 and shown in Figs. 5 and 6, respectively. It can be seen that both of Ni(II) and Co(II)

complexes are coordinated by four water molecules and two monodentate L ligands, while hydrogen-bonded interactions of the coordinated water molecules with sulfonic oxygen atoms of naphthalene-2-sulfate anions are observed, which are coincident with the coordination configuration of Ni(II) and Co(II) complexes as reported in Refs. [14, 16]. Important bond lengths (Å) and angles (°) of optimized $Ni[L_2(H_2O)_4](DNNS)_2$ and $Co[L_2(H_2O)_4](DNNS)_2$ in the gas phase were listed in Table S1 and Table S2, respectively. The bond lengths and angles in the optimized Ni(II) and Co(II) complexes varies slightly from the lengths and angles in the single crystals of the Ni(II) and Co(II) model complexes as reported in Refs. [14, 16]. The deviation in the geometrical parameters is due to the fact that the DFT calculations are done for an isolated molecule in the gaseous phase while the X-ray crystallographic data are obtained from the crystal lattice of the metal complexes. According to the structural parameters of the Ni(II) and Co(II) complexes, the lengths of Ni–O bonds (2.079 Å and 2.106 Å) have a lower value than those of Co–O bonds (2.099 Å and 2.122 Å), while the length of the Ni–N bond (2.154 Å) is found to be shorter than that of the Co–N bond (2.216 Å). It can be deduced that the Ni(II) and Co(II) complexes have similar stoichiometries, but more covalence contraction of the Ni(II) complex manifests in shorter bonds than that of the Co(II) complex.

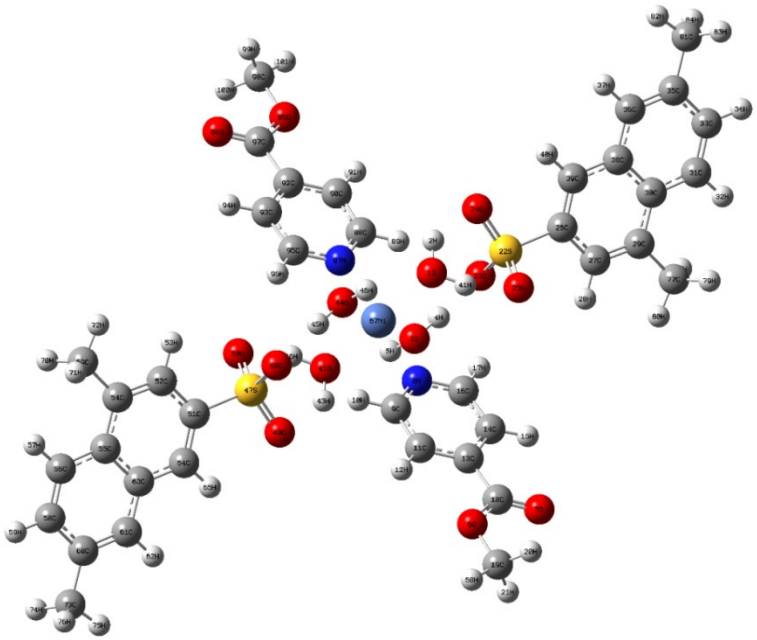

Fig. 5 Optimized structures of $Ni[L_2(H_2O)_4](DNNS)_2$ in the gas phase

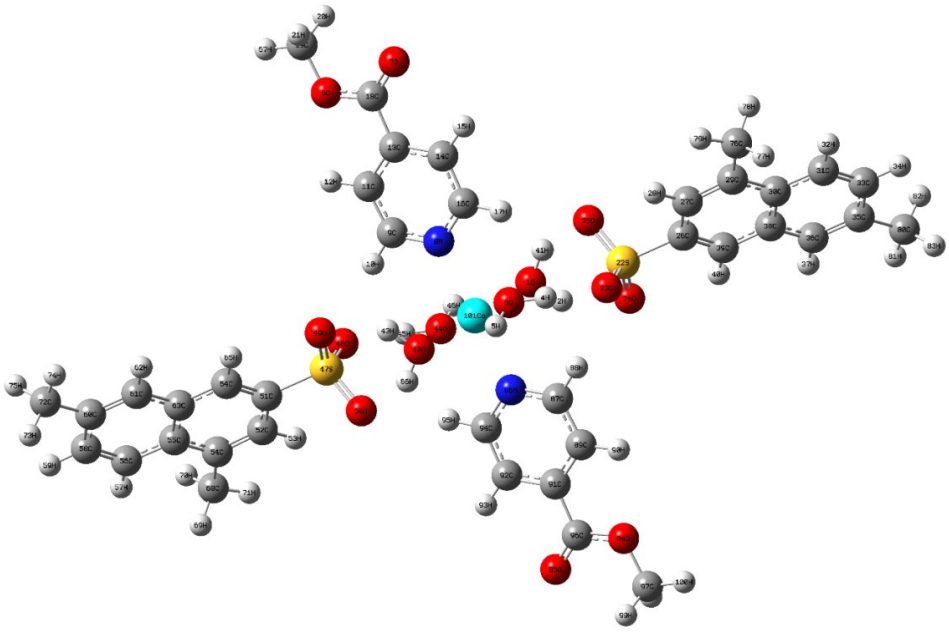

Fig. 6 Optimized structures of $Co[L_2(H_2O)_4](DNNS)_2$ in the gas phase

3.5 Thermodynamics for the hydration of Ni(II) and Co(II)

The structures of Ni(II) and Co(II) cations in aqueous solutions have been studied by experimental and theoretical methods [30, 31]. $[Ni(H_2O)_6]^{2+}$ and $[Co(H_2O)_6]^{2+}$ were considered as the most favorable species, the structures of which

were optimized in the gas phase and the aqueous solution (Fig. S1 and Table S3). As listed in Table S3, the calculated lengths of Ni–O and Co–O bonds are in agreement with the experimental data [32-34], as the average deviations are correspondingly 0.006 Å and 0.011 Å. The energy parameters, including zero-point energies (E), Gibbs free energies (G) and enthalpies (H) for the related species in the gas phase and the aqueous solution were obtained based on the frequency analysis (Table S4 and Table S5). Accordingly, the gas-phase change of Gibbs free energy for the hydration of M^{2+} (where M=Ni or Co) to form the species $[M(H_2O)_6]^{2+}$, $\Delta G_{(gas)}$, is determined according to the following equation:

$$\Delta G_{(gas)} = G_{(gas)}[M(H_2O)_6{}^{2+}] - 6G_{(gas)}[(H_2O)] - G_{(gas)}[M^{2+}] \quad (7)$$

Where, $G_{(gas)}[M(H_2O)_6{}^{2+}]$, $G_{(gas)}[(H_2O)]$, and $G_{(gas)}[M^{2+}]$ are the respective Gibbs free energies of the species of $M(H_2O)_6{}^{2+}$, H_2O and M^{2+} in the gas phase.

The aqueous-phase change in Gibbs free energy for the hydration of M^{2+} after considering the solvation effects, $\Delta G_{(hyd)}$, is further calculated based on a thermodynamical cycle proposed by other authors [35-37]. By using the thermodynamical cycle in Fig.7, $\Delta G_{(hyd)}$ is calculated by

$$\Delta G_{(hyd)} = \Delta G_{(gas)} + \Delta G_{(sol)}[M(H_2O)_6{}^{2+}] - 6\Delta G_{(sol)}[(H_2O)] - \Delta G_{(sol)}[M^{2+}] \quad (8)$$

Where, $\Delta G_{(sol)}[M(H_2O)_6{}^{2+}]$, $\Delta G_{(sol)}[(H_2O)]$, and $\Delta G_{(sol)}[M^{2+}]$ are the respective solvation energies of the species $M(H_2O)_6{}^{2+}$, H_2O and M^{2+}.

Then, the differences in the aqueous-phase changes of Gibbs free energies for the hydration of Ni(II) and Co(II), $\Delta\Delta G_{(hyd)}$, is obtained according to the following equation:

$$\Delta\Delta G_{(hyd)} = \Delta G_{(hyd)}[Ni] - \Delta G_{(hyd)}[Co] \quad (9)$$

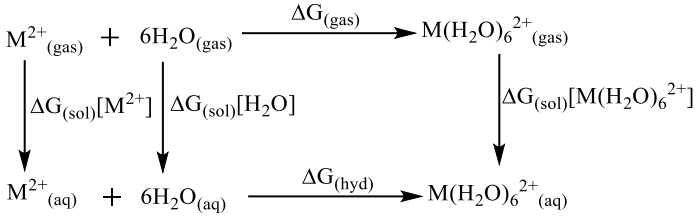

Fig. 7 Thermodynamical cycle for the hydration of the cations M^{2+} (M=Ni or Co)

The obtained thermodynamical parameters for the hydration reactions of Ni(II) and Co(II) were shown in Table 1.

Table 1. Thermodynamical parameters (kcal·mol^{-1}) for the hydration reaction of Ni(II) and Co(II) in the gas phase and the aqueous solution

Hydration reaction	$\Delta H_{(gas)}$	$\Delta S_{(gas)}$/cal·(mol·K)$^{-1}$	$\Delta G_{(gas)}$	$\Delta G_{(hyd)}$	$\Delta\Delta G_{(hyd)}$
$Ni^{2+} + 6H_2O \rightarrow [Ni(H_2O)_6]^{2+}$	-398.62	-188.66	-342.37	-502.62	-15.01
$Co^{2+} + 6H_2O \rightarrow [Co(H_2O)_6]^{2+}$	-388.88	-189.43	-332.40	-487.61	

Statistical solvation thermodynamics for ions has been discussed in the studies of Ben-Naim [38] and Marcus [39]. According to Ref.[40], the experimentally obtained values of $\Delta G_{(hyd)}[Ni]$ and $\Delta G_{(hyd)}[Co]$ are -473.23 and -457.70 kcal·mol^{-1}, which means that the experimentally obtained value of $\Delta\Delta G_{(hyd)}$ is -15.53 kcal·mol^{-1}. Meanwhile, the theoretically calculated values of $\Delta G_{(hyd)}[Ni]$ and $\Delta G_{(hyd)}[Co]$, are -502.62 and -487.61 kcal·mol^{-1}, which has absolute errors of -29.39 kcal·mol^{-1} for Ni(II) and -29.91 kcal·mol^{-1} for Co(II) in comparison with the experimentally obtained values. However, the theoretically calculated value of $\Delta\Delta G_{(hyd)}$ (-15.01 kcal·mol^{-1}) is very close to the experimentally obtained $\Delta\Delta G_{(hyd)}$ value (-15.53 kcal·mol^{-1}). Therefore, it is considered to be acceptable to apply the thermodynamical cycle for the examination of energy contribution for the difference of the formation of Ni(II) and Co(II) complexes with similar stoichiometries. On the basis of the

thermodynamical cycles, thermodynamics for the synergistic extraction reactions of Ni(II) and Co(II) were further examined.

3.6 Thermodynamics for the synergistic extraction of Ni(II) and Co(II)

The geometry configurations of all the related species were firstly optimized, and the corresponding energy parameters were listed in Table S6. Accordingly, the gas-phase changes in enthalpy ($\Delta H_{(gas)}$), entropy ($\Delta S_{(gas)}$), and Gibbs free energy ($\Delta G_{(gas)}$) were calculated, and the respective changes in Gibbs free energies for the synergistic extraction reactions of Ni(II) and Co(II) in the aqueous solution, $\Delta G_{(ext)}$, were calculated based on the thermodynamical cycle presented in Fig. 8.

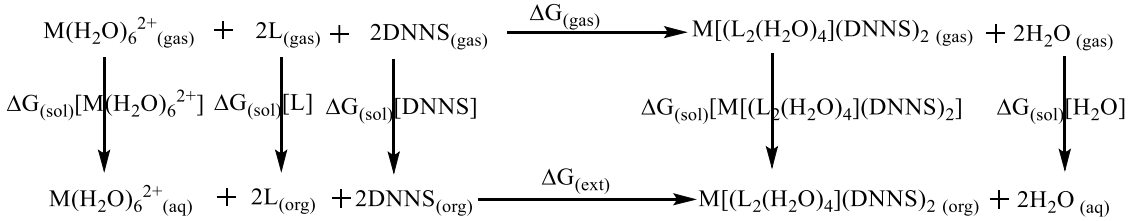

Fig. 8 Thermodynamical cycles for the extraction of M^{2+} (M=Ni or Co) with the synergistic extractant containing HDNNS and the ligand L.

In the thermodynamical cycle shown in Fig.8, $\Delta G_{(ext)}$ is calculated by

$$\Delta G_{(ext)} = \Delta G_{(gas)} + \Delta G_{(sol)}[M[L_2(H_2O)_4](DNNS)_2] + 2\Delta G_{(sol)}[H_2O] - \Delta G_{(sol)}[M(H_2O)_6{}^{2+}] - 2\Delta G_{(sol)}[L] - 2\Delta G_{(sol)}[DNNS] \quad (10)$$

Where, $\Delta G_{(sol)}[M[L_2(H_2O)_4](DNNS)_2$, $\Delta G_{(sol)}[(H_2O)]$, $\Delta G_{(sol)}[M(H_2O)_6{}^{2+}]$, $\Delta G_{(sol)}[L]$, and $\Delta G_{(sol)}[DNNS]$, are the solvation energies of $M[L_2(H_2O)_4](DNNS)_2$, H_2O and $M(H_2O)_6{}^{2+}$, ligand L and the deprotonated HDNNS, respectively.

$\Delta G_{(gas)}$ is obtained according to the following equation:

$$\Delta G_{(gas)} = G_{(gas)}[M[L_2(H_2O)_4](DNNS)_2] + 2G_{(gas)}[H_2O] - G_{(gas)}[M(H_2O)_6{}^{2+}] - 2G_{(gas)}[L] - 2G_{(gas)}[DNNS] \quad (11)$$

To further examined to assess the selectivity towards Ni(II) over Co(II) with the synergistic extractant, the difference in the aqueous-phase changes of Gibbs free energies for the synergistic extractions of Ni(II) and Co(II), $\Delta\Delta G_{(ext)}$, is determined according to the following equations:

$$\Delta\Delta G_{(ext)} = \Delta G_{(ext)}[Ni] - \Delta G_{(ext)}[Co] \quad (12)$$

The obtained thermodynamical parameters for the extraction reactions of Ni(II) and Co(II) were shown in Table 2.

Table 2. Thermodynamical parameters (kcal·mol^{-1}) for the extraction reactions of Ni(II) and Co(II) in the gas phase and the aqueous solution

Extraction reaction	$\Delta H_{(gas)}$	$\Delta S_{(gas)}$/Cal·(mol·K)$^{-1}$	$\Delta G_{(gas)}$	$\Delta G_{(ext)}$	$\Delta\Delta G_{(ext)}$
$Ni(H_2O)_6{}^{2+} + 2L + 2DNNS \rightarrow Ni[L_2(H_2O)_4](DNNS)_2 + 2H_2O$	-306.82	-107.78	-274.69	-260.14	-5.67
$Co(H_2O)_6{}^{2+} + 2L + DNNS \rightarrow Co[L_2(H_2O)_4](DNNS)_2 + 2H_2O$	-298.95	-102.10	-268.51	-254.47	

As listed in Table 2, $\Delta G_{(gas)}$ values are calculated as -274.69 kcal·mol^{-1} for the extraction of Ni(II) and -268.51 kcal·mol^{-1} for the extraction of Co(II). Meanwhile, according to the thermodynamical cycle in Fig. 8, the values of $\Delta G_{(ext)}$ for the extractions of Ni(II) and Co(II) in the aqueous solution are correspondingly -260.14 and -254.47 kcal·mol^{-1}, which are lower than those in the gas phase. It can be inferred that it is quite different for the Ni(II) and Co(II) extractions in the gas phase and in the aqueous solution after considering the solvation effects. The theoretically calculated $\Delta\Delta G_{(ext)}$value is obtained as -5.67 kcal·mol^{-1} (that is -23.74 kJ·mol^{-1}), which is close

414 to the experimental observations (-14.78 kJ·mol^{-1}) in this paper. This agreement
415 indicates that the complex stoichiometry and energy contribution are important for the
416 synergistic extractions of Ni(II) and Co(II). However, it is worth noticing that the
417 practical synergistic extraction process is much more complicated. For instance, the
418 reverse micelles would form in the loaded organic phase, which has been detected in
419 our previously reported studies [41]. Therefore, the contributions of other interactions,
420 e.g., the role of aggregation, which is so far insufficiently examined, would be the
421 focus of the ongoing research.

422

423 **4. Conclusions**

424 This study explored the extractability of Ni(II) and Co(II) with synergistic
425 extractant containing aryl sulfonates and monodentate aromatic nitrogen donor ligand
426 via experimental measurements as well as theoretical calculations. It has
427 demonstrated that both of Ni(II) and Co(II) had affinities with the synergistic
428 extractant and the possibilities to be extracted directly and simultaneously from highly
429 acidic sulfate solution. However, Ni(II) extraction appeared distinctly preferential
430 extractability compared that of Co(II) in the whole experimental range. DFT
431 calculations further revealed the intrinsic relation between microstructure and energy
432 contributions for understanding the extraction difference. According to the optimized
433 geometry configuration, similar coordination chemistry between Ni(II) and Co(II)
434 complexes was found but the shorter Ni–O and Ni–N bonds implied that the nickel
435 complexes would be more stable than cobalt complexes in the gas phase. Both

436 statistical thermodynamics analysis and DFT calculations indicated that the Gibbs free
437 energy change of the formation of the Ni(II) complex was more negative than that of
438 Co(II), indicating that the synergistic extractant containing HDNNS and the ligand L
439 was preferred to coordinate with Ni(II) than Co(II). Therefore, theoretical analysis of
440 metal-ligand bonding coordination and energy information would contribute to
441 preliminary understanding of the origin of preferential extraction of Ni(II) towards
442 Co(II) in synergistic extraction process.

443

444 **Acknowledgements**

445 This work was supported by the National Basic Research Program of China
446 (No.2014CB643401), the National Natural Science Foundation of China (Nos.
447 51134007 and 51674294), the Hunan Provincial Science and Technology Plan Project,
448 China (Nos. 2016TP1007, 2017TP1001, and 2019JJ30031), the Fundamental
449 Research Funds for the Central Universities of Central South University and the
450 Chinese Scholarship Council. Besides, we gratefully acknowledge helpful comments
451 and suggestions from anonymous reviews.

452

453 **References**

454 [1] C.Y. Cheng, K.R. Barnard, W. Zhang, D.J. Robinson, Synergistic solvent extraction of nickel
455 and cobalt: a review of recent developments, Solvent Extr. Ion Exc., 29 (2011) 719-754.
456 [2] C.Y. Cheng, Solvent extraction of nickel and cobalt with synergistic systems consisting of
457 carboxylic acid and aliphatic hydroxyoxime, Hydrometallurgy, 84 (2006) 109-117.
458 [3] C.Y. Cheng, K.R. Barnard, W. Zhang, Z. Zhu, Y. Pranolo, Recovery of nickel, cobalt, copper and
459 zinc in sulphate and chloride solutions using synergistic solvent extraction, Chinese J. Chem.
460 Eng., 24 (2016) 237-248.
461 [4] M.P. Elizafde, M. Cox, M. Aguilar, Synergistic Extraction of Ni(II) by mixtures of Lix63 and

462 bis-(2-ethylhexyl)phosphoric or di-n-octylphosphinic acids in toluene, Solvent Extr. Ion Exc.,
463 14 (1996) 833-848.
464 [5] J.S. Preston, A.C.D. Preez, Synergistic effects in the solvent extraction of some divalent metals
465 by mixtures of versatic 10 acid and pyridinecarboxylate esters, J. Chem. Technol. Biotechnol.,
466 61 (2010) 159-165.
467 [6] M. Hutton-Ashkenny, D. Ibana, K.R. Barnard, Reagent selection for recovery of nickel and
468 cobalt from nitric acid nickel laterite leach solutions by solvent extraction, Miner. Eng., 77
469 (2015) 42-51.
470 [7] K. Osseo-asare, M.E. Keeney, Sulfonic Acids: Catalysts for the Liquid-Liquid Extraction of
471 Metals, Sep. Sci. Technol., 15 (2006) 999-1011.
472 [8] J.S. Preston, A.C. du Preez, Solvent extraction of nickel from acidic solutions using synergistic
473 mixtures containing pyridinecarboxylate esters. Part 3. Systems based on arylsulphonic acids,
474 J. Chem. Technol. Biotechnol., 71 (1998) 43-50.
475 [9] C.Y. Cheng, G. Boddy, W. Zhang, M. Godfrey, D.J. Robinson, Y. Pranolo, Z. Zhu, W. Wang,
476 Recovery of nickel and cobalt from laterite leach solutions using direct solvent extraction: Part
477 1 -selection of a synergistic SX system, Hydrometallurgy, 104 (2010) 45-52.
478 [10] C.Y. Cheng, G. Boddy, W. Zhang, M. Godfrey, D.J. Robinson, Y. Pranolo, Z. Zhu, L. Zeng, W.
479 Wang, Recovery of nickel and cobalt from laterite leach solutions using direct solvent
480 extraction, Hydrometallurgy, 104 (2010) 53-60.
481 [11] K. Osseo-Asare, D. Renninger, Synergic extraction of nickel and cobalt by
482 LIX63-dinonylnaphthalene sulfonic acid mixtures, Hydrometallurgy, 13 (1984) 45-62.
483 [12] B.P. Taili Zhou, A pyridine-based chelating solvent extraction system for selective extraction
484 of nickel and cobalt, Hydrometallurgy, 46 (1997) 37-53.
485 [13] A.I. Okewole, N.P. Magwa, Z.R. Tshentu, The separation of nickel(II) from base metal ions
486 using 1-octyl-2-(2′-pyridyl)imidazole as extractant in a highly acidic sulfate medium,
487 Hydrometallurgy, (2012) 81-89.
488 [14] S. Zhu, H. Hu, J. Hu, J. Li, F. Hu, Y. Wang, Structural insights into the extraction mechanism of
489 cobalt(II) with dinonylnaphthalene sulfonic acid and 2-ethylhexyl 4-pyridinecarboxylate ester,
490 J. Coord. Chem., (2018) 1-16.
491 [15] F. Hu, H. Hu, Y. Luo, Y. Wang, J. Yang, J. Hu, The separation of Ni(II) over base metal ions in
492 acidic polymetallic medium: Synergistic extraction and structural evidence, Hydrometallurgy,
493 181 (2018) 240-247.
494 [16] J. Li, H. Hu, S. Zhu, F. Hu, Y. Wang, The coordination structure of the extracted nickel(ii)
495 complex with a synergistic mixture containing dinonylnaphthalene sulfonic acid and
496 2-ethylhexyl 4-pyridinecarboxylate ester, Dalton Trans., 46 (2017) 1075-1082.
497 [17] H.H. F. Hu, J. Hu, S. Zhu, J. Yang, Y. Wang, Improving selective separation of Cu(II) from
498 acidic polymetallic media with 2-ethylhexyl 4-pyridinecarboxylate ester: extraction behaviors,
499 coordination structure and microscopic mechanism, J. Mol. Liq., 248 (2017) 1050-1058.
500 [18] O.T.J. Bertrán, Solvent effects and chemical reactivity, (2002).
501 [19] J.M. Keith, E.R. Batista, Theoretical examination of the thermodynamic factors in the selective
502 extraction of Am^{3+} from Eu^{3+} by dithiophosphinic acids, Inorg. Chem., 51 (2012) 13-15.
503 [20] C. Xiaoyan, H. Daniel, C. Jan, D. Michael, First-principles study of the separation of
504 Am(III)/Cm(III) from Eu(III) with Cyanex301, Inorganic Chemistry, 49 (2010) 10307.
505 [21] J.-H. Lan, W.-Q. Shi, L.-Y. Yuan, J. Li, Y.-L. Zhao, Z.-F. Chai, Recent advances in

computational modeling and simulations on the An(III)/Ln(III) separation process, Coord. Chem. Rev., 256 (2012) 1406-1417.
[22] J. Narbutt, W.P. Oziminski, Selectivity of bis-triazinyl bipyridine ligands for americium(III) in Am/Eu separation by solvent extraction. Part 1. Quantum mechanical study on the structures of BTBP complexes and on the energy of the separation, Dalton Trans., 41 (2012) 14416-14424.
[23] J.S. Preston, A.C.d. Preez, The solvent extraction of nickel and cobalt bymixtures of carboxylic acids and pyridinecarboxylate esters, Solvent Extr. Ion Exc., 13 (1995) 465-494.
[24] C. Lee, W. Yang, R.G. Parr, Development of the Colle-Salvetti correlation-energy formula into a functional of the electron density, Phys. Rev. B Condens. Matter., 37 (1988) 785-789.
[25] A.D. Becke, Density-functional thermochemistry. III. The role of exact exchange, J. Chem. Phys., 98 (1993) 5648-5652.
[26] J.R. Frisch, G.W. Trucks, H.B. Schlegel, G.E. Scuseria, M.A. Robb, J.R. Cheeseman, V.G. Zakrewski, J.A. Montgomery, R.E. Stratmann, J.C.D.S. Burant, Gaussian 03, revision C. 02; Gaussian, Inc.: Wallingford, CT,, (2004).
[27] C. Reichardt, T. Welton, Solvents and solvent effects in organic chemistry, John Wiley & Sons, 2011.
[28] H. Junming, K. Andreas, M.L. Coote, Comment on the correct use of continuum solvent models, J. Phys. Chem. A, 114 (2010) 13442-13444.
[29] A.V. Marenich, C.J. Cramer, D.G. Truhlar, Performance of SM6, SM8, and SMD on the SAMPL1 test set for the prediction of small-molecule solvation free energies, J. Phys. Chem. B, 113 (2009) 4538.
[30] N. Zhang, D. Zeng, J. Brugger, Q. Zhou, Y. Ngothai, Effect of Solvent Activity on Solute Association: The Formation of Aqueous Nickel(II) Chloride Complexes Studied by UV–Vis and EXAFS Spectroscopy, J. Solution Chem., 44 (2015) 1320-1338.
[31] T.J. Swift, The Kinetics of Structural Transformation of Hydrated Cobalt(II) and Zinc(II) Ions in Aqueous Solution, Inorg. Chem., 3 (1964).
[32] M. Magini, Hydration and complex formation study on concentrated MCl2 solutions [M=Co(II), Ni(II), Cu(II)] by x-ray diffraction technique, J. Chem. Phys., 74 (1981) 2523-2529.
[33] Y. Marcus, Ionic radii in aqueous solutions, Journal of Solution Chemistry, 12 (1983) 271-275.
[34] W. Bol, G.J.A. Gerrits, C.L.V.P. Eck, The hydration of divalent cations in aqueous solution. An X-ray investigation with isomorphous replacement, J. Appl. Crystallogr., 3 (2010) 486-492.
[35] V.S. Bryantsev, M.S. Diallo, W.A. Goddard, Calculation of solvation free energies of charged solutes using mixed cluster/continuum models, J. Phys. Chem. B, 112 (2008) 9709-9719.
[36] X. Cao, D. Heidelberg, J. Ciupka, M. Dolg, First-principles study of the separation of Am(III)/Cm(III) from Eu(III) with Cyanex301, Inorg. Chem, 49 (2010) 10307-10315.
[37] J. Ciupka, X. Cao-Dolg, J. Wiebke, M. Dolg, Computational study of lanthanide(III) hydration, Phys Chem Chem Phys, 12 (2010) 13215-13223.
[38] A. Ben-Naim, Solvation thermodynamics of water in aqueous solutions. I. Theory and limiting effect of solutes, J. Chem. Phys., 82 (1985) 4662-4667.
[39] Y. Marcus, Ions in Solution and their Solvation, 2015.
[40] Y. Marcus, Thermodynamics of solvation of ions. Part 5.—Gibbs free energy of hydration at 298.15 K, J. Chem. Soc., Faraday T., 87 (1991) 2995-2990.

[41] Y. Luo, H. Hu, Y. Wang, F. Hu, S. Zhu, S. Zhang, Y. Zhang, S. Li, J. Wang, Phase separation in solvent extraction of copper or nickel from acidic solution using a sulfonic acid (HDNNS) and a carboxylate ester (4PC), J. Dispersion Sci. Technol., (2018) 1-9.